

Generating macroscopic-quantum-superposition states in momentum and internal-state space from Bose-Einstein condensates with repulsive interactions

J. Higbie and D. M. Stamper-Kurn

Department of Physics, University of California, Berkeley, California 94720, USA

(Received 23 October 2003; published 7 May 2004)

Resonant Raman coupling between internal levels can create double-well momentum-space potentials for multilevel “periodically-dressed” atoms. We develop a many-body formalism for a weakly interacting, trapped periodically dressed Bose gas which illustrates how a tunable exchange interaction yields correlated many-body ground states. In contrast to the case of a position-space double well, the ground state of stable periodically-dressed Bose gases with repulsive interactions tends toward a macroscopic superposition state in the regime where interactions dominate the momentum-space tunneling induced by the external trapping potential. We discuss how real-time control of experimental parameters can be used to create macroscopic quantum superpositions of either momentum or internal states, and how these states could be dynamically controlled, opening the way toward highly sensitive interferometry and frequency metrology.

DOI: 10.1103/PhysRevA.69.053605

PACS number(s): 03.75.Gg, 05.30.Jp, 52.38.Bv

Following our mastery over the internal and external states of individual atoms, the scientific frontier advances to the full control over the quantum states of many-body systems. Entangled states, in which the constituents of a many-body system display nonclassical correlations, play a key role in our developing understanding of quantum information and decoherence, and may find practical use in quantum communication [1], quantum computing, and high-precision metrology [2–5]. Various techniques are being developed that generate entanglement deterministically in, for example, spin-squeezed atomic ensembles [6], trapped ions [7], the electromagnetic field [8], and superconducting circuits [9,10].

Ultracold neutral atoms offer a promising route to generating highly entangled many-body states. Schemes for generating such entanglement rely on interatomic interactions which provide “nonlinear” elements as seen from the viewpoint of single-particle dynamics. Such nonlinear terms are provided naturally through binary collisions between ground-state atoms, as utilized controllably by Mandel *et al.* [11], and can be further enhanced through molecular resonances or by the assistance of near-resonant photons [12,13].

A paradigmatic system in which interatomic interactions induce entanglement is a collection of ultracold interacting bosons in a parity-symmetric double-well potential [14–17]. The lowest-energy single-particle states are the parity-even ground state $|\psi_0\rangle$ and parity-odd first excited state $|\psi_1\rangle$, separated in energy by the tunnel splitting J . If tunneling and interactions are weak with respect to the energy spacings to other single-particle states, the many-body system may be described by the two-mode Hamiltonian

$$\mathcal{H} = -\frac{J}{2}(\hat{c}_R^\dagger \hat{c}_L + \hat{c}_L^\dagger \hat{c}_R) - U \hat{N}_R \hat{N}_L, \quad (1)$$

whence terms dependent only on the total number of atoms in the system are omitted. Here \hat{c}_R and \hat{c}_L denote annihilation operators for particles in the right ($|R\rangle = [|\psi_0\rangle + |\psi_1\rangle]/\sqrt{2}$) or left ($|L\rangle = [|\psi_0\rangle - |\psi_1\rangle]/\sqrt{2}$) well states, respectively. The

number operators $\hat{N}_R = \hat{c}_R^\dagger \hat{c}_R$ and $\hat{N}_L = \hat{c}_L^\dagger \hat{c}_L$ count particles in the right and left wells, respectively, of the double-well system. The parameter U gives the energy due to short-range interactions of a pair of atoms located in the same well.

This simple Hamiltonian leads to highly correlated many-body ground states through the interplay of tunneling and interaction. One finds three limiting behaviors. If the tunneling rate dominates, the many-body ground-state of N bosons is driven to the factorized, uncorrelated state in which all N atoms are identically in the single-particle ground state $|\psi_0\rangle$. In the limit $N|U|/J \gg 1$, the interaction energy dominates. For repulsive interactions ($U > 0$), a many-body state divides itself evenly between the two potential minima, generating the state $|\Psi\rangle \propto (\hat{c}_R^\dagger)^{N/2} (\hat{c}_L^\dagger)^{N/2} |0\rangle$, where $|0\rangle$ is the vacuum state. Experimental evidence for such a “number-squeezed” state has been obtained by Orzel *et al.* in a many-well potential [18]. Similar physics is responsible for the observed Mott-insulator phase in a three-dimensional periodic potential [19].

For attractive interactions ($U < 0$), the ground state is quite spectacular: a macroscopic-quantum-superposition (Schrödinger-cat) state $|\Psi\rangle \propto [(\hat{c}_R^\dagger)^N + (\hat{c}_L^\dagger)^N] |0\rangle$ formed as a superposition of states in which *all* atoms are found in one of the two wells. The generation of Schrödinger-cat states is a tantalizing goal; at present, the largest atomic Schrödinger-cat states contain just four atoms [7]. However, accomplishing this goal by imposing a double-well potential on a collection of bosons with attractive interactions is a daunting task: such Bose-Einstein condensates are unstable to collapse [20], implying that the number of bosons placed into the superposition state will be small; moreover, exceptional spatial control over trapping potentials and over the interaction strength is required.

The above discussion pertains to atoms for which the *position-space potential is a double well*, while the kinetic-energy term $p^2/2m$ may be regarded as a *momentum-space harmonic potential*. In this work, we point out that an analogous many-body system can be crafted, in which the roles of

position and momentum are interchanged. As discussed in previous work [21–23], the dispersion relation of multilevel atoms placed in a spatially periodic coupling between internal states can take the form of a momentum-space double-well potential. Addition of a *harmonic position-space trapping potential* produces a double-well system dual to that discussed above. Assessing the roles of interparticle interactions in this situation, we find that the many-body ground states for bosonic atoms in such a system are highly entangled in both momentum and internal-state space. In opposition to the situation of bosons in position-space double wells, maximally entangled states may be generated in the case of *repulsive* interactions, allowing the creation of such states starting with large, stable Bose-Einstein condensates while obviating the need for exacting control over potentials with extremely small spatial dimensions.

The roles of repulsive or attractive interactions in determining the behavior of interacting bosons in momentum-space double-well potentials are reversed from those in the case of position-space potentials. As discussed below, this reversal is due to an exchange term which arises in the evaluation of the interaction energy of a Bose gas that occupies several distinct momentum states. For repulsive interactions, for example, this exchange term disfavors a macroscopic occupation of more than one single-particle wave function (the so-called fractionation of a condensate as discussed by Leggett [24] and others), thus favoring a Schrödinger-cat superposition. We find that the strength of the exchange term can be dynamically varied by varying parameters of the periodic coupling field which generates the double-well potential.

Following a derivation of the momentum-space double-well potential (Sec. I), we develop a two-mode approximate treatment of this system which provides expressions for the interaction and tunneling energies and thereby clarifies their dependence on experimental parameters (Sec. II). Similar work by Montina and Arecchi [23] treats this system using the Gross-Pitaevskii equation as the starting point, a numerical scheme which identifies the onset of correlated many-body ground states. Their work appears to reproduce our analytic approach in the limit of weak interactions, while the validity of their approach (or, indeed, any extant treatment) for stronger interactions is difficult to establish. Furthermore, in Sec. III, we show that maximal entanglement can be generated purely between internal states or between momentum states, offering a route to Heisenberg-limited atomic clocks [3] or atomic interferometry [5], respectively.

I. ORIGIN OF THE MOMENTUM-SPACE POTENTIAL

We consider bosonic atoms of mass m with two internal states $|A\rangle$ and $|B\rangle$ at energies $\hbar\omega_A$ and $\hbar\omega_B$, respectively. These atoms are exposed to laser fields of frequencies ω_1 and ω_2 ($\omega = \omega_1 - \omega_2$) and wave vectors \mathbf{k}_1 and \mathbf{k}_2 which induce Raman transitions between the two internal states [see Figs. 1(a) and 1(b)]. Thus, a Raman process from state $|A\rangle$ to $|B\rangle$ imparts a momentum of $\hbar\mathbf{k} = \hbar(\mathbf{k}_1 - \mathbf{k}_2)$ and kinetic energy of $\hbar\delta = \hbar\omega - \hbar(\omega_B - \omega_A)$. The continuous Raman coupling can be regarded as a spatially periodic coupling field between the internal states of the atoms, represented by an off-diagonal

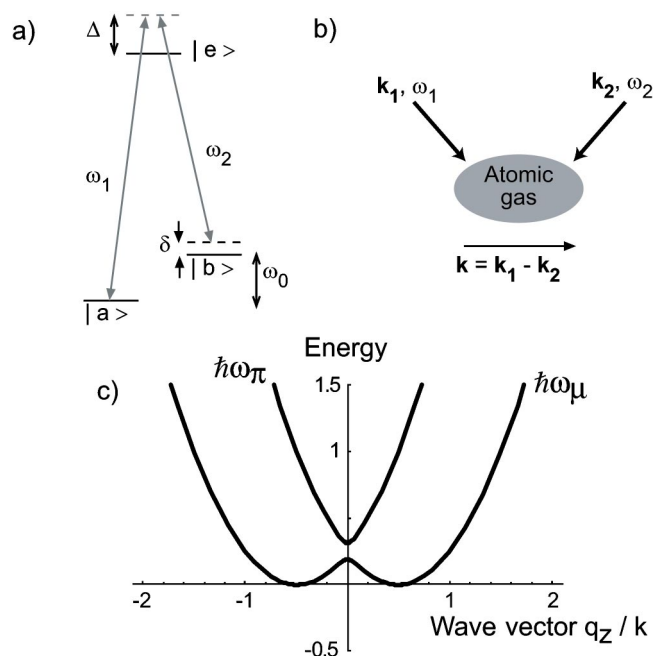


FIG. 1. Creating a double-well momentum-space potential with Raman excitation. (a) Laser beams of frequency ω_1 and ω_2 may induce Raman transitions between internal states $|A\rangle$ and $|B\rangle$. $\delta = (\omega_1 - \omega_2) - \omega_0$ is the detuning from the Raman resonance. (b) Such a Raman transition imparts a momentum transfer of $\hbar\mathbf{k} = \hbar(\mathbf{k}_1 - \mathbf{k}_2)$, where \mathbf{k}_1 and \mathbf{k}_2 are the wave vectors of the Raman coupling lasers. (c) Atoms exposed to continuous Raman excitation can be described by a two-branch dispersion relation. Energies (scaled by E_k) for the lower ($\hbar\omega_\mu$) and upper ($\hbar\omega_\pi$) dressed states are shown for wave vectors (scaled by k) in the direction of the Raman momentum transfer. In the case of exact Raman resonance ($\delta=0$) and small Raman Rabi frequency (shown for $\hbar\Omega/E_k=1/8$), the lower dispersion relation takes the form of a parity-symmetry double-well potential.

potential $V_R = \hbar\Omega/2(e^{-i(\mathbf{k}\cdot\mathbf{r}-\omega t)}|A\rangle\langle B| + e^{i(\mathbf{k}\cdot\mathbf{r}-\omega t)}|B\rangle\langle A|)$. Here Ω is the two-photon Rabi frequency, taken to be real, which is determined by dipole matrix elements, the detuning from intermediate resonances, and by the laser intensities.

It is convenient to analyze this constantly driven system in terms of “periodically-dressed” states, which are coherent superpositions of both internal and external (momentum) states. As developed in Refs. [21,22], this treatment reveals marked anisotropy and tunability in the superfluid characteristics of a Bose-Einstein condensate formed of such a dressed-state gas. Given a two-component spinor wave function $\tilde{\psi}(\mathbf{r}) = [\psi_A(\mathbf{r}), \psi_B(\mathbf{r})]$ to describe single-atom states in the $\{|A\rangle, |B\rangle\}$ basis, we transform to a frame which is *corotating* and *comoving* with the driving laser fields, yielding a spinor wave function $\tilde{\psi}(\mathbf{r})$ with components $\tilde{\psi}_{A,B}(\mathbf{r}) = \exp[\pm i(\mathbf{k}\cdot\mathbf{r} - \omega t)/2]\psi_{A,B}(\mathbf{r})$. This transformation yields a Schrödinger equation with two de Broglie wave solutions at each momentum $\hbar\mathbf{q}$, which we call the periodically-dressed states. The two-branch dispersion relation of the periodically-dressed atoms has the form (using π for plus and μ for minus)

$$\hbar\omega_{\pi,\mu}(\mathbf{q}) = q^2 + \frac{1}{4} \pm \frac{1}{2} \sqrt{(2\mathbf{q} \cdot \mathbf{k} - \delta)^2 + \Omega^2}, \quad (2)$$

where energies and wave vectors are scaled by the Raman recoil energy $E_k = \hbar^2 k^2 / 2m$ and wave vector k , respectively.

Under the conditions of exact Raman resonance ($\delta=0$) and sufficiently small Rabi frequency Ω , a degeneracy of momentum ground states occurs as the lower dispersion relation takes the form of a double-well potential, with minima at $\pm \mathbf{Q}/2$ ($\mathbf{Q} \approx \mathbf{k}$) [Fig. 1(c)]. This potential can be quickly tuned by modifying the laser parameters. The detuning from Raman resonance δ breaks the ground-state degeneracy, favoring the right- or left-well states. The spacing between the potential wells is controlled by the Raman momentum transfer $\hbar\mathbf{k}$, which can be varied by reorienting the laser beams. Finally, the Rabi frequency Ω changes both the height of the barrier between the wells as well as the internal-state character of states on either side of the well [22].

In the case of a position-space double well, the kinetic energy of the atoms forbids a complete localization of atoms in either of the wells, thus introducing tunneling. Similarly, in our case of the momentum-space double well, a tunneling between well-defined momentum states can be induced by adding a spatially dependent term to the Hamiltonian. We consider adding an internal-state independent trapping potential of the form $V(\mathbf{r}) = m\omega_l^2 r^2 / 2$ [25]. The Hamiltonian for this system may be written in the basis of the periodically-dressed states introduced earlier, using the expansion

$$\tilde{\psi}(\mathbf{r}, t) = \int \frac{d^3\mathbf{q}}{(2\pi)^{3/2}} \mathbf{R}(\mathbf{q}) \begin{pmatrix} \pi(\mathbf{q}) \\ \mu(\mathbf{q}) \end{pmatrix} e^{i\mathbf{q}\cdot\mathbf{r}}, \quad (3)$$

where $\mathbf{R}(\mathbf{q}) = e^{-i\sigma_y \theta(\mathbf{q})/2}$, where σ_y is a Pauli matrix and the mixing angle $\theta(\mathbf{q})$ is defined by the relation $\cot \theta(\mathbf{q}) = (\delta - \hbar\mathbf{q} \cdot \mathbf{k} / m) / \Omega$. The wave function $\tilde{\phi}(\mathbf{q}) = (\pi(\mathbf{q}), \mu(\mathbf{q}))$ in the space of periodically-dressed momentum eigenstates obeys a Schrödinger equation with Hamiltonian

$$\hat{\mathcal{H}}_{PD} = \hbar \begin{pmatrix} \omega_+(\mathbf{q}) & 0 \\ 0 & \omega_-(\mathbf{q}) \end{pmatrix} - \frac{1}{M^2} \mathbf{R}^\dagger(\mathbf{q}) \nabla_q^2 \mathbf{R}(\mathbf{q}). \quad (4)$$

The position-space trapping potential is seen in momentum space as a kinetic-energy-like term (involving ∇_q^2), which accounts also for the variations with \mathbf{q} of the periodically-dressed eigenstate basis. The relevance of this kinetic-energy-like term is measured by the dimensionless effective mass parameter M , which is related to the Lamb-Dicke parameter $\eta = \sqrt{\hbar k^2 / 2m\omega_l}$ as $M = 2\eta^2$. For weak spatial confinement ($M \gg 1$), the low-energy single-particle states are restricted primarily to the lower periodically-dressed states, with the two lowest states split by a small tunneling energy J . For strong confinement ($M \ll 1$), the single-particle states are admixtures of upper- and lower-dispersion-relation periodically-dressed states, and a simple double-well treatment is no longer adequate.

To introduce interatomic interactions, we make use of the field operator $\hat{\phi}(\mathbf{q}) = (\hat{\pi}(\mathbf{q}), \hat{\mu}(\mathbf{q}))$ the components of which annihilate particles in the lower (μ) or upper (π) periodically-dressed states. These operators obey Bose com-

mutation relations. We consider low-energy, binary, elastic collisions with a state-independent scattering length a .

The interaction Hamiltonian then takes the form $\hat{\mathcal{H}}_{\text{int}} = (g/2) [\int d^3\mathbf{q} \hat{n}(\mathbf{q}) \hat{n}(-\mathbf{q})]$, neglecting terms dependent only on the total number of atoms N , where $\hat{n}(\mathbf{q})$ is the spatial Fourier transform of the density operator, and $g = 8\pi k a$ is the properly scaled interaction parameter. The density operator is given as [21,22]

$$\hat{n}(\mathbf{q}) = \int \frac{d^3\kappa}{(2\pi)^{3/2}} \hat{\phi}^\dagger\left(\kappa + \frac{\mathbf{q}}{2}\right) \mathbf{R}^\dagger\left(\kappa + \frac{\mathbf{q}}{2}\right) \mathcal{R}\left(\kappa - \frac{\mathbf{q}}{2}\right) \hat{\phi}\left(\kappa - \frac{\mathbf{q}}{2}\right). \quad (5)$$

II. THE TWO-MODE APPROXIMATION

To simplify our treatment, let us consider only the situation in which the two lowest-energy eigenvalues (in the absence of interactions) are well separated from the remaining energies, and thus a two-mode description of the many-body system is adequate. The two lowest-energy single-particle states have wave functions $\tilde{\phi}_0(\mathbf{q})$ and $\tilde{\phi}_1(\mathbf{q})$, mode operators \hat{c}_0 and \hat{c}_1 , and energy splitting J . We define the right- and left-well states as $\tilde{\phi}_{R,L}(\mathbf{q}) = [\tilde{\phi}_0(\mathbf{q}) \pm \tilde{\phi}_1(\mathbf{q})] / \sqrt{2}$, and the mode operators as $\hat{c}_{R,L} = (\hat{c}_0 \pm \hat{c}_1) / \sqrt{2}$. Under this approximation, we can evaluate the density operator $\hat{n}(\mathbf{q})$ by expanding the field operators $\hat{\mu}(\mathbf{q})$ and $\hat{\pi}(\mathbf{q})$ in the basis of energy eigenstates, and then truncating the expansion after the first two states. We then express the density operator as $\hat{n}(\mathbf{q}) \approx \sum_{i,j} \mathcal{N}_{ij}(\mathbf{q}) \hat{c}_i^\dagger \hat{c}_j$ with

$$\mathcal{N}(\mathbf{q})_{ij} = \int \frac{d^3\kappa}{(2\pi)^{3/2}} \tilde{\phi}_i^\dagger\left(\kappa + \frac{\mathbf{q}}{2}\right) \mathcal{R}\left(\kappa + \frac{\mathbf{q}}{2}\right) \mathcal{R}\left(\kappa - \frac{\mathbf{q}}{2}\right) \times \tilde{\phi}_j\left(\kappa - \frac{\mathbf{q}}{2}\right), \quad (6)$$

with indices $i, j \in \{R, L\}$ denoting either the right or left states. Accounting for properties of the right- and left-well states under parity [26], we obtain

$$\hat{n}(\mathbf{q}) \approx \mathcal{N}_{RR}(\mathbf{q}) N + \mathcal{N}_{RL}(\mathbf{q}) \hat{c}_R^\dagger \hat{c}_L + \mathcal{N}_{RL}(-\mathbf{q}) \hat{c}_L^\dagger \hat{c}_R, \quad (7)$$

where N is the total number of atoms in the system. Dropping terms that depend only on N , one thus finds

$$\hat{\mathcal{H}}_{\text{int}} \approx -U \hat{N}_R \hat{N}_L + \frac{J_1}{2} (\hat{c}_R^\dagger \hat{c}_L + \hat{c}_L^\dagger \hat{c}_R) + J_2 (\hat{c}_R^\dagger \hat{c}_R^\dagger \hat{c}_L \hat{c}_L + \hat{c}_L^\dagger \hat{c}_L^\dagger \hat{c}_R \hat{c}_R), \quad (8)$$

where the energies U , J_1 , and J_2 are given as

$$U = -g \int d^3\mathbf{q} \mathcal{N}_{RL}^2, \quad (9)$$

$$J_1 = 2Ng \int d^3\mathbf{q} \mathcal{N}_{RR}(\mathbf{q}) \mathcal{N}_{RL}(\mathbf{q}), \quad (10)$$

$$J_2 = \frac{g}{2} \int d^3\mathbf{q} \mathcal{N}_{RL}(\mathbf{q}) \mathcal{N}_{RL}(-\mathbf{q}). \quad (11)$$

Before delving further into the implications of the interaction Hamiltonian given above, let us consider the weak-confinement (large M) limit at which the right- and left-well states contain no population in the upper (π) dressed states, are Gaussian functions well localized (in \mathbf{q} space) at the right and left potential minima at $\pm\mathbf{Q}/2$, with rms widths $\sigma_q \approx (2M)^{-1/2}$, and have average density per particle $\langle n \rangle = \sigma_q^3 / \pi^{3/2}$. In calculating the integrals of Eq. (6), we may thus use local values of the rotation matrices $\mathcal{R}(\mathbf{q})$ at $\pm\mathbf{Q}/2$, as appropriate. We then find

$$U = -g \langle n \rangle \sin^2 \theta \left(\frac{\mathbf{Q}}{2} \right), \quad (12)$$

$$J_1 = 2Ng \langle n \rangle \sin \theta \left(\frac{\mathbf{Q}}{2} \right) e^{-Q^2/16\sigma_q^2}, \quad (13)$$

$$J_2 = \frac{g}{2} \langle n \rangle \sin^2 \theta \left(\frac{\mathbf{Q}}{2} \right) e^{-Q^2/4\sigma_q^2}. \quad (14)$$

These approximations can be further simplified by setting $\mathbf{Q} = \mathbf{k}$, and thus $\sin \theta(\mathbf{Q}/2) \approx \sqrt{\Omega^2/(1+\Omega^2)}$.

Let us presume that the interaction-mediated tunneling terms J_1 and J_2 are negligibly small. We thus recover the many-body Hamiltonian of Eq. (1) which had applied to the position-space double well. However, examining the interaction energy U , we now find that *the roles of attractive and repulsive interactions are interchanged* between the position-space and momentum-space double-well treatments: for the case of the momentum-space double-well potential, repulsive interactions ($g > 0$) yield $U < 0$ and thus are the source of Schrödinger-cat ground states, while attractive interactions ($g < 0$) yield $U > 0$ and thus are the source of number-squeezed ground states. This opens the door to the production of Schrödinger-cat states for large, robust Bose-Einstein condensates with repulsive interactions through the use of binary collisions as a nonlinear coupling.

This reversal of roles for repulsive and attractive interactions in momentum space can be understood in the context of a single-component Bose-Einstein condensate in a harmonic potential. Repulsive interactions lead the ground-state condensate wave function to become larger spatially, thus causing the momentum-space wave function to contract—appearing as an attractive interaction in momentum space. Equivalently, one may note that in a Hartree approximation to the many-body state of a Bose-Einstein condensate, the interaction energy is evaluated as an interaction energy density proportional to the square of the density. The density of a Bose gas occupying two distinct momentum states would be spatially modulated by the interference between the momentum states, and, therefore, its interaction energy $\propto gn^2$ would be increased (decreased) for the case of repulsive (attractive) interactions. Thus we find repulsive interactions leading to Schrödinger-cat states, a superposition of states in which only one single-particle state is macro-

scopically occupied, while attractive interactions would lead to a “fractionation” of the condensate between distinct momentum states.

In the system we have described here, the interaction energy U is a *tunable exchange term* which, in the case of repulsive interactions, suppresses the superposition of atoms in two distinct momentum states and thereby favors the maximally entangled state. The exchange term in the interaction Hamiltonian arises from the presence of atoms in identical internal states, but different momentum states. By adjusting the strength of the Rabi coupling Ω , the admixture of internal states $|A\rangle$ and $|B\rangle$ in the right- and left-well states is varied. For small Ω , atoms in the right-well state are almost purely in the $|A\rangle$ state, and atoms in the left-well state are almost purely in the $|B\rangle$ state. Thus, the strength of the exchange term is suppressed [$\sin^2 \theta(\mathbf{Q}/2) \ll 1$], and the product state $|\Psi\rangle \propto (\hat{c}_R + \hat{c}_L)^N |0\rangle$ remains energetically favored. For larger Ω , the right- and left-well states both contain admixtures of the two internal states; e.g., the right-well state contains atoms in state $|A\rangle$ nearly at rest, while the left-well state contains atoms in state $|A\rangle$ at momentum $\sim -\hbar\mathbf{k}$. Significant exchange terms now suppress the product state in favor of the maximally entangled state.

The dependence of the many-body ground state on the ratio U/J and the atom number N has been worked out by various authors [14,16,17] for the position-space double-well potential. As we have obtained a Hamiltonian identical in form to the position-space treatment, these predictions would apply directly to our scheme. Significant deviations from the factorized, noninteracting atom solution begin at $|U/J| \gtrsim 1/N$; for repulsive ($U > 0$) or attractive ($U < 0$) interactions this would shift population either away from or towards the state $|N_L = N/2, N_R = N/2\rangle$, respectively. Perturbation analysis shows that the many-body state will be well approximated by the Schrödinger-cat state $(|N, 0\rangle + |0, N\rangle) / \sqrt{2}$ when $U/J > 1/\sqrt{N}$.

Now returning to Eq. (8), we see that two extra terms appear in $\hat{\mathcal{H}}_{\text{int}}$ which do not conserve the number of particles in the right- and left-well states, representing a form of interaction-mediated tunneling. The first, involving $J^{(1)}$, modifies the tunneling energy between the right and left wells. The effect of this term is to reduce the tunneling rate for repulsive interactions, and increase it for attractive interactions. This can be understood by noting that repulsive interactions tend to raise the energy of the single-particle ground state more than the first excited state since the ground state has a higher density. Our previous analysis of the two-mode approximation accommodates this term by a redefinition of J as $J \rightarrow J - J^{(1)}$, leading to no further complications. The second tunneling term, involving $J^{(2)}$, describes collisions which can redistribute two atoms from the right well to the left well, and vice versa. While this term modifies the conclusions of our simple treatment, we have seen that the magnitudes of both $J^{(1)}$ and $J^{(2)}$ are exponentially suppressed with respect to U , and thus the dominant role of interactions is to create the aforementioned many-body ground states. These terms will, however, play an important role in determining the strength of interactions at which many-body correlations begin to become evident; the scaling of J (independ-

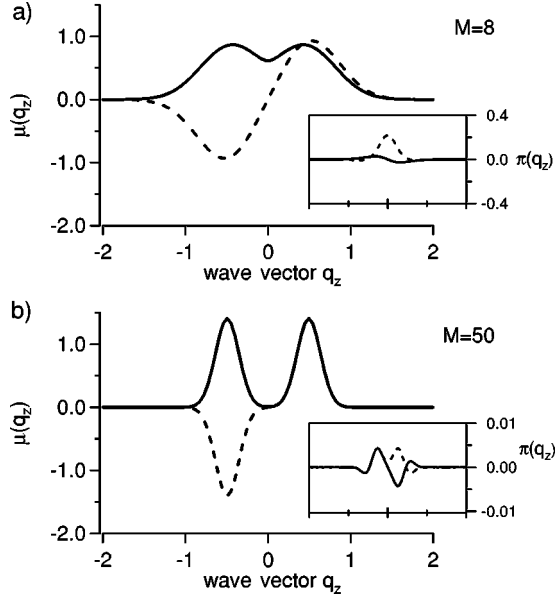


FIG. 2. The two lowest-energy eigenfunctions (solid line for the ground state and dashed for the excited state) which define the right- and left-well modes for the two-mode approximation. Component wave functions in the lower $[\mu(q_z)]$ and upper $[\pi(q_z)]$, shown in insets] periodically dressed states are shown for $M=8$ and $M=50$. As the spatial confinement is weakened (larger M), the wave functions become further localized in the minima of the double-well potential, and the population in the upper dressed state diminishes. Note the different parity of the μ and π components, as discussed in the text. Here $\hbar\Omega/E_k=1/8$, wave vectors are scaled by k , and the one-dimensional wave functions $\vec{\phi}_{0,1}(q_z)$ are shown.

dent of g), $J^{(1)}$, $J^{(2)}$, and U with the control parameters (Ω , g , M , etc.) are different and thereby provide more tunability to the system.

We performed numerical calculations of the lowest-energy single-particle states to verify the simple scaling behavior of various terms in the Hamiltonian described above. The single-particle Hamiltonian of Eq. (4) is separable in the three Cartesian coordinates defined so that one axis (say \hat{z}) lies along the direction of the Raman momentum transfer \mathbf{k} . We then have the lowest-energy eigenstates as $\vec{\phi}_{0,1}(\mathbf{q}) = \vec{\phi}_{0,1}(q_z)\exp[-(q_x^2 + q_y^2)/4\sigma_q^2]/\sqrt{2\pi\sigma_q^2}$, a product of harmonic-oscillator ground states in the \hat{x} and \hat{y} directions and normalized solutions $\vec{\phi}_{0,1}(q_z)$ to the one-dimensional, two-component Schrödinger equation derived from Eq. (4).

These one-dimensional eigenstates, calculated using a restricted basis set of Fourier components over the domain $-3 \leq q \leq 3$, are shown in Fig. 2 for two different values of the mass parameter M , and for the condition of exact Raman resonance $\delta=0$ and Rabi frequency $\hbar\Omega/E_k=1/8$. For weak spatial confinement (large $M=50$), the lowest two energy eigenstates are indeed nearly entirely composed of lower dressed states ($\pi(q_z) \approx 0$) and are well approximated by the sum or difference of Gaussian right- and left-well wave functions centered at the potential minima near $q_z/k \approx \pm 1/2$. For stronger spatial confinement (smaller $M=8$), the enhanced “momentum-space tunneling” causes the wave functions to become less confined in the potential minima. Concomi-

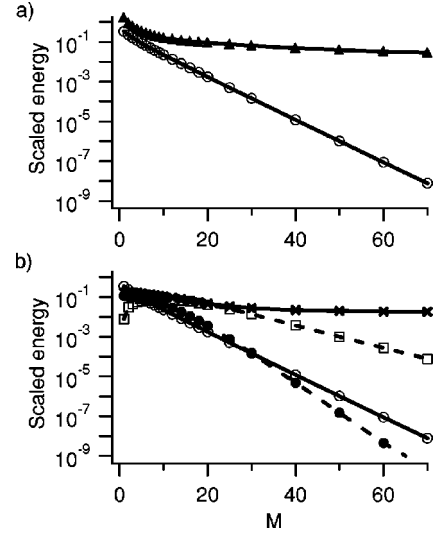


FIG. 3. Numerical calculations of tunneling and interaction strengths. (a) The tunnel splitting J (open circles, solid line) becomes much smaller than the spacing between the second and third excited states (open triangles, solid line) for moderate values of M , establishing the validity of the two-mode approximation for weak confinement. (b) Tunneling energies J (open circles, solid line), $J^{(1)}$ (open squares, dashed line), and $J^{(2)}$ (filled circles, dashed line) are suppressed for weaker confinement (exponentially with large M), while the strength of the momentum exchange energy U (\times 's, solid line) remains large. This provides a route to creating correlated many-body states adiabatically from uncorrelated states by gradually weakening the spatial confinement. The energies in (a) are scaled by E_k . Dimensionless interaction parameters are plotted as $-U/g\langle n \rangle$, $J^{(1)}/2Ng\langle n \rangle$, $J^{(2)}/(g\langle n \rangle/2)$. A Rabi frequency $\hbar\Omega/E_k=1/8$ is chosen.

tantly, a significant population appears in the upper dressed states.

Parameters which enter into the two-mode Hamiltonian are derived from the numerically obtained wave functions, and are shown in Fig. 3. One finds the scaling $J \sim \exp(-M/4)$ as one expects [27]. The numerical results confirm the scaling behavior for $J^{(1)}$ found in the weak-confinement (large M) limit [Eqs. (12)–(14)], but differ slightly from the scaling predicted for $J^{(2)}$ since the assumption that the right-well state remains Gaussian in the vicinity of the left-well potential minimum is incorrect. Nevertheless, $J^{(2)}$ is strongly suppressed for large M , approximately as $\exp(-M/3)$. Also shown is the energy splitting between the second and third lowest eigenenergies; one sees that for weak spatial confinement the lowest two energy eigenstates become well separated from the remaining eigenspectrum, establishing the validity of the two-mode approximation.

Finally, we stress that the two-mode treatment presented here becomes invalid in the Thomas-Fermi regime, where the strength of atomic interactions dominates the zero-point energy in the confining potential. In this situation, additional single-particle states must be considered, resulting in a complicated, self-consistent definition of the right- and left-well states which depends on the number of atoms in these states. How to properly treat such a situation remains an open question, and therefore an important subject for experimental in-

vestigation. In related work, Montina and Arecchi [23] obtain right- and left-well states through use of the Gross-Pitaevskii equation, but the validity of their treatment is questionable for systems which are not completely interaction dominated.

III. APPLICATION TO HEISENBERG-LIMITED MEASUREMENT

Several theoretical works have pointed out the potential for correlated many-body states for improving the precision of atomic clocks [4] and interferometers [5,28], in which phase shifts are measured at the Heisenberg limit $\Delta\phi \propto 1/N$, rather than the standard quantum limit $\Delta\phi \propto 1/\sqrt{N}$, where N is the number of particles used in a single run of the experiment. In particular, Bollinger *et al.* described the use of the maximally entangled state in such a measurement [4]. In this section, we point out how dynamical control over experimental parameters can be used fruitfully to generate Schrödinger-cat states suited for the implementation of both Heisenberg-limited spectroscopy and interferometry.

In the system we have described, repulsive interatomic interactions lead to lowest-energy many-body states which are the even- and odd-superposition Schrödinger-cat states $|S_{\pm}\rangle = (|\Psi_R\rangle \pm |\Psi_L\rangle)/\sqrt{2}$. The states $|\Psi_R\rangle$ and $|\Psi_L\rangle$ are distinguishable many-body states associated with the right and left potential wells, respectively, which tend toward the limiting cases $|\Psi_R\rangle \rightarrow |0, N\rangle$ and $|\Psi_L\rangle \rightarrow |N, 0\rangle$ for strong interactions. The energy separation between these two states depends on the residual overlap between $|\Psi_R\rangle$ and $|\Psi_L\rangle$ and the number of atoms in the system (derived, e.g., in Ref. [15]). In the weak-confinement limit $M \gg 1$, these right- and left-well states are composed of the lower dressed states, which are superpositions in both internal and external degrees of freedom. Such a superposition appears to complicate the use of these Schrödinger-cat states for measurement applications.

However, after these Schrödinger-cat states are formed, the dressed right- and left-well states *can be converted to pure internal or external states adiabatically*, i.e., by modification of experimental parameters on a time scale which is fast with respect to tunneling times so as to preserve entanglement, but slow with respect to time scales relevant to the Raman coupling ($1/\Omega$). If the Rabi frequency Ω is adiabatically lowered to zero (the Raman beams are slowly extinguished), atoms in the right-well state would be adiabatically converted to stationary trapped atoms in the $|A\rangle$ internal state, while atoms in the left well would be converted to stationary trapped atoms in the $|B\rangle$ state. Thus would be prepared a state ideal for Heisenberg-limited measurement of the internal-state energy difference $\hbar\omega_0$, potentially on a useful hyperfine clock transition. Alternately, one could adiabatically ramp the detuning from the Raman resonance to large positive or negative values. For example, an adiabatic downward sweep of the frequency difference between the Raman laser beams ($\delta \rightarrow -\infty$) lowers the energy of the $|A\rangle$ internal state with respect to the $|B\rangle$ internal state in the rotating frame. This adiabatically converts the right- and left-well states to *distinguishable momentum states* with identical internal states (in this case the $|A\rangle$ state). One thereby pre-

pares a state ideal for Heisenberg-limited atomic interferometry.

Furthermore, the timed application of Raman coupling in this system can be used as a “magic beam splitter” [29] to prepare the Schrödinger-cat state dynamically. For simplicity let us make the identification $|\Psi_R\rangle = |0, N\rangle$ and $|\Psi_L\rangle = |N, 0\rangle$. Consider a system prepared in the $|\Psi\rangle = |N, 0\rangle$ state with no Raman coupling ($\Omega=0$)—this state corresponds to a zero-temperature Bose-Einstein condensate of N atoms in the $|B\rangle$ internal state. The Raman coupling is then turned on adiabatically, as discussed above. The initial state $|\Psi\rangle$, being a superposition of the two lowest-energy Schrödinger-cat energy eigenstates, is now led to oscillate coherently, and collectively, between the right- and left-well states. This oscillation is analogous to macroscopic quantum tunneling observed, for example, in the Rabi oscillations of superconducting qubits [30]. If the Raman coupling is left on for a duration which is $1/4$ of the Bohr period between the even and odd Schrödinger-cat states, the many-body state $|\Psi\rangle$ will evolve as

$$|\Psi\rangle \rightarrow \frac{|S_+\rangle - i|S_-\rangle}{\sqrt{2}} = \frac{1-i}{2}|N, 0\rangle + \frac{1+i}{2}|0, N\rangle. \quad (15)$$

The Raman beams can be then switched off—with the transformation of the state into a momentum space or internal-state-space Schrödinger-cat state, as desired—for a duration τ , during which a relative phase can accrue between the two distinguishable portions of the Schrödinger-cat state, i.e.,

$$|\Psi\rangle \rightarrow \frac{1-i}{2}|N, 0\rangle + \frac{1+i}{2}e^{-iN\Delta\tau}|0, N\rangle. \quad (16)$$

Here Δ is the difference in energy between the single-particle states to which the right- and left-well states are connected when the Raman beams are extinguished. For instance, if we are following the implementation of a measurement of the clock frequency between internal states, $\Delta = \delta$.

Finally, this state must be analyzed. In the scheme of Bollinger *et al.* [4], a conventional $\pi/2$ pulse is applied, and a precise measurement is made of the difference between the number of atoms in the $|A\rangle$ state and the $|B\rangle$ state—one must establish whether this number difference is even or odd, thus requiring single-atom precision in the number counting.

Alternately, one may apply a *second* magic beam splitter pulse as before, thus preparing a state

$$|\Psi\rangle \rightarrow \frac{-i(1 - e^{-iN\Delta\tau})}{2}|N, 0\rangle + \frac{(1 + e^{-iN\Delta\tau})}{2}|0, N\rangle. \quad (17)$$

Measurements on this state would detect *all atoms* in either the right- or left-well states (say, internal states $|A\rangle$ or $|B\rangle$), with probabilities which vary periodically with the free-evolution time τ with frequency $N\Delta$ which is N times higher than for a single-particle Ramsey-type measurement. This is the source of the enhanced Heisenberg-level sensitivity. This sensitivity persists even in the presence of overall number fluctuations, presuming that one’s goal is to ascertain whether $\Delta=0$. However, the correct timing required to yield a perfect magic beam splitter will depend on N [15]. Thus,

attaining the highest precision will still require a highly accurate determination of the total atom number N , though perhaps not necessarily at the single-atom level. A promising avenue for precise atom-number determination and deterministic initial-state preparation is the use of a high-finesse optical cavity, whose spectrum depends sensitively on the number of atoms in the cavity [31]. Alternatively (or equivalently in the case of cavity enhancement), the number could be obtained nondestructively from phase-contrast imaging of the atomic sample. Measuring the total number before entangling the many-body state in the first beam splitter offers the advantage of eliminating measurement-induced decoherence as a limiting factor in the lifetime of the macroscopic superposition. Its disadvantage is that the atom number may diminish subsequent to the initial measurement. Avoiding such a decrease, however, is unlikely to impose any severe additional constraint on the number-loss rate, given that the Schrödinger-cat states are already very sensitive to decoherence via number loss. A further unexamined issue is how the finite temperature of the atomic sample, which prevents the initial state $|\Psi\rangle$ from being a pure Bose-Einstein condensate, will affect the precision of these Schrödinger-cat-based measurements.

In conclusion, we have presented an analytic model which identifies the many-body ground states of a weakly interacting Bose gas which is periodically dressed by continuous

Raman excitation and confined in a harmonic spatial potential. The system is analyzed in momentum space, wherein the balance between tunneling and weak interactions dictates whether the ground states are uncorrelated product states of single-particle wave functions, or highly correlated states. It is found that interactions in the physical system considered here have the opposite effect as in the dual situation of a position-space double-well potential, that is, repulsive interactions will lead to Schrödinger-cat states while attractive interactions will lead to number-squeezed states with equal numbers of atoms in each well. Further, we show that experimental parameters can be used to dynamically tune the interaction strength and tunneling rates. This degree of control can be used to generate maximally entangled states directly suitable for Heisenberg-limited metrology and interferometry.

ACKNOWLEDGMENTS

We thank Lorraine Sadler, Subhadeep Gupta, Joel Moore, and Veronique Savalli for critical discussions and reading. This work was supported by the National Science Foundation under Grant No. 0133999, by the Hellman Faculty Fund, the Sloan Foundation, the Packard Foundation, and the University of California.

-
- [1] C. H. Bennett *et al.*, Phys. Rev. Lett. **70**, 1895 (1993).
 - [2] C. M. Caves, Phys. Rev. D **23**, 1693 (1981).
 - [3] D. J. Wineland *et al.*, Phys. Rev. A **46**, R6797 (1992).
 - [4] J. J. Bollinger *et al.*, Phys. Rev. A **54**, R4649 (1996).
 - [5] P. Bouyer and M. A. Kasevich, Phys. Rev. A **56**, R1083 (1997).
 - [6] B. Julsgaard *et al.*, Nature (London) **413**, 400 (2001).
 - [7] C. A. Sackett *et al.*, Nature (London) **404**, 256 (2000).
 - [8] M. Brune *et al.*, Phys. Rev. Lett. **77**, 4887 (1996).
 - [9] Y. A. Pashkin *et al.*, Nature (London) **421**, 823 (2003).
 - [10] A. J. Berkley *et al.*, Science **300**, 1548 (2003).
 - [11] O. Mandel *et al.*, Nature (London) **425**, 937 (2003).
 - [12] A. André and M. D. Lukin, Phys. Rev. A **65**, 053819 (2002).
 - [13] A. S. Sorensen and K. Molmer, Phys. Rev. A **66**, 022314 (2002).
 - [14] A. Imamoglu *et al.*, Phys. Rev. Lett. **78**, 2511 (1997).
 - [15] J. I. Cirac *et al.*, Phys. Rev. A **57**, 1208 (1998).
 - [16] J. Javanainen and M. Y. Ivanov, Phys. Rev. A **60**, 2351 (1999).
 - [17] R. W. Spekkens and J. E. Sipe, Phys. Rev. A **59**, 3868 (1999).
 - [18] C. Orzel *et al.*, Science **291**, 2386 (2001).
 - [19] M. Greiner *et al.*, Nature (London) **415**, 39 (2002).
 - [20] C. A. Sackett *et al.*, Phys. Rev. Lett. **82**, 876 (1999).
 - [21] J. Higbie and D. M. Stamper-Kurn, Phys. Rev. Lett. **88**, 090401 (2002).
 - [22] D. M. Stamper-Kurn, New J. Phys. **5**, 50 (2003).
 - [23] A. Montina and F. T. Arecchi, Phys. Rev. A **67**, 23616 (2003).
 - [24] A. J. Leggett, Rev. Mod. Phys. **73**, 307 (2001).
 - [25] Such a potential for ultracold alkali-metal atoms might be created by optical trapping at large detunings and/or with linearly polarized light, or by magnetic trapping of two states with identical magnetic moments. For simplicity, we have also chosen a radially symmetric trap, though our analysis is only slightly modified by trap asymmetry as long as the Raman momentum transfer $\hbar\mathbf{k}$ is aligned along an axis of the trap.
 - [26] Defining the operator $\mathcal{P}^* = \mathcal{P}\sigma_z$, where \mathcal{P} is the parity operator and σ_z the Pauli matrix, we find for $\delta=0$ that $[\mathcal{P}^*, \hat{\mathcal{H}}]=0$. Given $\phi_{0,1}^{PD}$ are real, we obtain the relations $\mathcal{N}_{RR}(\mathbf{q}) = \mathcal{N}_{LL}(\mathbf{q}) = \mathcal{N}_{RR}(-\mathbf{q})$ and $\mathcal{N}_{RL}(\mathbf{q}) = \mathcal{N}_{LR}(-\mathbf{q})$.
 - [27] A similar scalar one-dimensional double-well potential—two offset parabolas connected with a discontinuous slope—is treated analytically as a textbook problem. See, for example, E. Merzbacher, *Quantum Mechanics*, 2nd ed. (Wiley, New York, 1970), Eq. 5.61.
 - [28] M. J. Holland and K. Burnett, Phys. Rev. Lett. **71**, 1355 (1993).
 - [29] H. Lee *et al.*, J. Mod. Opt. **49**, 2325 (2002).
 - [30] I. Chiorescu *et al.*, Science **299**, 1868 (2003).
 - [31] S. Leslie *et al.*, Phys. Rev. A **69**, 043805 (2004).